

New spectroscopic confirmations of Lyman- α emitters at $z \sim 7$ from the LAGER survey

SANTOSH HARISH,¹ ISAK G. B. WOLD,² SANGEETA MALHOTRA,² JAMES RHOADS,² WEIDA HU,^{3,4} JUNXIAN WANG,^{3,4} ZHEN-YA ZHENG,⁵ L. FELIPE BARRIENTOS,⁶ JORGE GONZÁLEZ-LÓPEZ,^{7,6} LUCIA A. PEREZ,¹ ALI AHMAD KHOSTOVAN,² LEOPOLDO INFANTE,⁸ CHUNYAN JIANG,⁵ CRISTÓBAL MOYA-SIERRALTA,⁶ JOHN PHARO,¹ FRANCISCO VALDES,⁹ AND HUAN YANG⁸

¹*School of Earth and Space Exploration, Arizona State University, Tempe, AZ 85287, USA*

²*Astrophysics Science Division, NASA Goddard Space Flight Center, 8800 Greenbelt Road, Greenbelt, Maryland, 20771, USA*

³*CAS Key Laboratory for Research in Galaxies and Cosmology, Department of Astronomy, University of Science and Technology of China, Hefei, Anhui 230026, People's Republic of China*

⁴*School of Astronomy and Space Science, University of Science and Technology of China, Hefei 230026, People's Republic of China*

⁵*CAS Key Laboratory for Research in Galaxies and Cosmology, Shanghai Astronomical Observatory, Shanghai 200030, People's Republic of China*

⁶*Instituto de Astrofísica, Facultad de Física, Pontificia Universidad Católica de Chile, Santiago, Chile*

⁷*Núcleo de Astronomía de la Facultad de Ingeniería y Ciencias, Universidad Diego Portales, Av. Ejército Libertador 441, Santiago, Chile*

⁸*Las Campanas Observatory, Carnegie Institution of Washington, Casilla 601, La Serena, Chile*

⁹*National Optical Astronomy Observatory, 950 N. Cherry Avenue, Tucson, AZ 85719, USA*

ABSTRACT

We report spectroscopic confirmations of 15 Lyman-alpha galaxies at $z \sim 7$, implying a spectroscopic confirmation rate of $\sim 80\%$ on candidates selected from LAGER (Lyman-Alpha Galaxies in the Epoch of Reionization), which is the largest (24 deg^2) survey aimed at finding Lyman-alpha emitters (LAEs) at $z \sim 7$ using deep narrow-band imaging from DECam at CTIO. LAEs at high-redshifts are sensitive probes of cosmic reionization and narrow-band imaging is a robust and effective method for selecting a large number of LAEs. In this work, we present results from the spectroscopic follow-up of LAE candidates in two LAGER fields, COSMOS and WIDE-12, using observations from Keck/LRIS. We report the successful detection of Ly α emission in 15 candidates (11 in COSMOS and 4 in WIDE-12 fields). Three of these in COSMOS have matching confirmations from a previous LAGER spectroscopic follow-up and are part of the overdense region, LAGER- $z7OD1$. Additionally, two candidates that were not detected in the LRIS observations have prior spectroscopic confirmations from Magellan. Including these, we obtain a spectroscopic confirmation success rate of $\sim 80\%$ for LAGER LAE candidates. Apart from Ly α , we do not detect any other UV nebular lines in our LRIS spectra; however, we estimate a 2σ upper limit for the ratio of NV/Ly α , $f_{NV}/f_{Ly\alpha} \lesssim 0.27$, which implies that ionizing emission from these sources is mostly dominated by star formation. Including confirmations from this work, a total of 33 LAE sources from LAGER are now spectroscopically confirmed. LAGER has more than doubled the sample of spectroscopically confirmed LAE sources at $z \sim 7$.

1. INTRODUCTION

Epoch of Reionization (EoR) marks a critical phase in the cosmic history when neutral hydrogen (HI) in the intergalactic medium (IGM) was ionized by intense UV radiation from sources such as star-forming galaxies and active galactic nuclei (AGN), soon after the dark ages. Recent efforts including Cosmic Microwave Background (CMB) observations by *Planck* (Planck Collaboration et al. 2016) and high-redshift quasar observa-

tions (e.g. Fan et al. 2006) suggest that the universe was highly ionized by $z \sim 6$; however, a detailed picture of the reionization process is still lacking, given significant challenges in observing the earliest sources in the universe. Among several observational probes that exist for studying reionization, Ly α emission from star-forming galaxies is one of the most powerful and sensitive tracer of HI in the IGM (e.g. Malhotra & Rhoads 2004, 2006; Stark et al. 2011; Pentericci et al. 2011; Dijkstra 2014; Zheng et al. 2017; Konno et al. 2018). Ly α photons undergo resonant scattering in the presence of HI and

therefore provide a reliable estimate of the HI fraction as the universe ionized.

Over the last two decades, a number of narrow-band (NB) imaging surveys have successfully selected large samples of Ly α emitters (LAEs) up to $z \sim 6$ (e.g. Rhoads et al. 2003, 2004; Malhotra & Rhoads 2004; Ouchi et al. 2005; Hu et al. 2010; Zheng et al. 2016). Some recent studies have found overdensities of Ly α (Zheng et al. 2017; Castellano et al. 2018; Hu et al. 2019, e.g.) and Lyman-break galaxies at $z \sim 7$ (e.g. Trenti et al. 2012; Castellano et al. 2016) which might indicate presence of large ionized regions. However, at $z \gtrsim 7$, attenuation of Ly α photons by the increasingly neutral IGM has resulted in fewer LAE candidates (e.g. Fontana et al. 2010; Treu et al. 2013; Pentericci et al. 2014; Mason et al. 2019) and shown a significant drop in terms of the Ly α luminosity function (e.g. Ota et al. 2010; Shibuya et al. 2012; Konno et al. 2014), compared to lower redshifts.

Lyman-Alpha Galaxies in the Epoch of Reionization (LAGER) is an ongoing, large NB survey searching for LAEs at $z \sim 7$, using the Dark Energy Camera (DECam) on the 4m Blanco telescope at Cerro Tololo Inter-American Observatory (CTIO), Chile (Zheng et al. 2017). LAGER employs a custom designed NB filter, NB964, with a central wavelength of 9642 Å.

In this paper, we present follow-up spectroscopic observations of several LAE candidates at $z \sim 7$ in COSMOS and WIDE-12 fields from the LAGER survey. Details of LRIS observations and the data reduction process is presented in Section 2. The resultant spectra and LAE identifications are shown in Section 3, followed by a summary in Section 4.

2. OBSERVATIONS AND DATA REDUCTION

2.1. Candidate LAE selection

Using the narrow-band filter NB964 (Zheng et al. 2019) – with a central wavelength of 9642Å and FWHM $\sim 90\text{Å}$ – on the Dark Energy Camera (DECam) mounted on the Blanco 4m telescope at CTIO, we have obtained 47.25 hours narrow-band exposure in the COSMOS field, reaching a 5σ detection limit of 25.2 mag ($2''$ aperture), and in WIDE-12 field, we have obtained 27.9 hours of narrow-band exposure reaching a 5σ detection limit of 24.7 mag ($1.8''$ aperture), as part of the LAGER survey. In COSMOS, LAE candidates at $z \sim 7$ were selected based on narrow-band flux excess (y - NB964 > 0.8) and non-detections in the bluer broad-band imaging (HSC g, r, i, z). The final sample contains 49 LAE candidates (for more details, see Hu et al. 2019). Similar approach was followed for the WIDE-12 region

Table 1. Keck/LRIS observation summary

Mask ID	Observation Date	No. of exposures $\times t_{exp}^{single}$ (s)	t_{exp}^{total} (h)	Seeing
WIDE12-19	Mar 5, 2019	$10 \times 900 + 1 \times 720$	2.7	$0.7''$
COSMOS-A-19	Mar 5, 2019	$10 \times 900 + 5 \times 600$	3.3	$0.7''$
COSMOS-B-19	Mar 5, 2019	7×720	1.4	$0.7''$
WIDE12-20	Jan 30, 2020	$16 \times 720 + 1 \times 600$	3.36	$0.6'' - 0.7''$
COSMOS-20	Jan 31, 2020	15×720	3	$0.5'' - 0.7''$

resulting in a sample of 50 LAE candidates (Wold et al. 2021).

2.2. LRIS spectroscopy

We observed 21 LAE candidates using the Low Resolution Imaging Spectrometer (LRIS) on the Keck I telescope (Oke et al. 1995; Rockosi et al. 2010) over one night in 2019 (March 5) and two half-nights in 2020 (January 30-31). With a beamsplitter in place, the red and blue cameras of LRIS can be operated simultaneously, providing a combined spectral coverage from 3200Å to 1 μm with a field-of-view of $6' \times 7.8'$. Given the expected redshifts of our candidate LAEs, we focus here on observations obtained by the red camera, which uses a mosaic of two LBNL 2k \times 4k CCD detectors, with a spatial resolution of $0.135''/\text{pixel}$. Our setup included the 400/8500 grating and a multi-slit mask. With our typical $1''$ slit width, this setup yields a spectral resolution of $\sim 7\text{Å}$. Each of our slitmasks in COSMOS and WIDE-12 fields included the $z \sim 7$ LAE candidates, foreground emission-line candidates, and alignment stars.

The 2019 observing run included three masks (2 in COSMOS and 1 in WIDE-12), covering a total of 15 LAE candidates, and the 2020 run included two masks (one each in COSMOS and WIDE-12), covering a total of 6 LAE candidates. Weather conditions were excellent in both runs with a seeing of $0.7''$ on March 5, 2019, and $0.5'' - 0.7''$ on January 30 – 31, 2020. The observation summary including number of exposures and total exposure time per mask is provided in Table 1.

2.3. Data Reduction

We reduced our LRIS observations using an open-source, Python-based data reduction pipeline called `PyPeIt` (Prochaska et al. 2020a,b). The reduction

Table 2. Properties of LAE candidates observed using Keck/LRIS

ID	Mask	R.A. (J2000)	Dec. (J2000)	z_{spec}	NB964 (mag)	$\log L_{Ly\alpha}^a$ (erg s $^{-1}$)
Confirmations						
J095933+014320	COSMOS-20	09:59:33.26	+01:43:20.42	6.923	24.82 ± 0.21	$42.84^{+0.08}_{-0.12}$
J095934+014406	COSMOS-20	09:59:34.80	+01:44:06.96	6.937	25.18 ± 0.23	$42.57^{+0.12}_{-0.19}$
J095954+013938	COSMOS-20	09:59:54.37	+01:39:38.33	6.930	25.0 ± 0.2	$42.73^{+0.09}_{-0.12}$
J095956+023259	COSMOS-A-19	09:59:56.04	+02:32:59.99	6.924	25.02 ± 0.2	$42.77^{+0.08}_{-0.12}$
J100000+023219	COSMOS-A-19	10:00:00.43	+02:32:19.27	6.926	24.43 ± 0.14	$42.99^{+0.06}_{-0.08}$
J100001+023402	COSMOS-A-19	10:00:01.84	+02:34:02.03	6.920	24.57 ± 0.21	$42.8^{+0.14}_{-0.19}$
J100012+023047	COSMOS-A-19	10:00:12.95	+02:30:47.26	6.929	23.61 ± 0.15	$43.31^{+0.07}_{-0.08}$
J100327+020851 ^b	COSMOS-B-19	10:03:27.99	+02:08:51.28	6.915	24.73 ± 0.23	$43.05^{+0.09}_{-0.12}$
J100332+020925 ^b	COSMOS-B-19	10:03:32.71	+02:09:25.11	6.898	24.33 ± 0.16	$43.04^{+0.06}_{-0.1}$
J100339+020747 ^b	COSMOS-B-19	10:03:39.32	+02:07:47.22	6.936	24.91 ± 0.22	$42.69^{+0.14}_{-0.2}$
J100339+020954	COSMOS-B-19	10:03:39.12	+02:09:54.42	6.920	25.49 ± 0.25	$42.55^{+0.11}_{-0.17}$
J120412-003157	WIDE12-20	12:04:12.68	-00:31:57.94	6.935	24.12 ± 0.07	$43.02^{+0.13}_{-0.18}$
J120406-002921	WIDE12-20	12:04:06.51	-00:29:21.40	6.907	24.44 ± 0.11	$42.93^{+0.18}_{-0.32}$
J120356-002648	WIDE12-20	12:03:56.77	-00:26:48.24	6.896	23.95 ± 0.06	$43.17^{+0.11}_{-0.14}$
J120637-001438	WIDE12-19	12:06:37.34	-00:14:38.95	6.929	24.25 ± 0.08	$43.02^{+0.14}_{-0.21}$
Interlopers						
J120636+000959	WIDE12-19	12:06:36.53	+00:09:59.07	0.925	24.21 ± 0.07	-
J120641-001047	WIDE12-19	12:06:41.19	-00:10:47.30	0.921	23.99 ± 0.06	-
Non-confirmations						
J100016+022847	COSMOS-A-19	10:00:16.94	+02:28:47.36	-	23.66 ± 0.13	$43.25^{+0.07}_{-0.09}$
J100333+020719 ^b	COSMOS-B-19	10:03:33.51	+02:07:19.80	-	24.61 ± 0.2	$42.94^{+0.07}_{-0.09}$
J100334+020909	COSMOS-B-19	10:03:34.63	+02:09:09.58	-	24.87 ± 0.21	$42.82^{+0.08}_{-0.12}$
J100337+020736 ^b	COSMOS-B-19	10:03:37.34	+02:07:36.65	-	24.81 ± 0.18	$42.86^{+0.06}_{-0.1}$

NOTE—^aPhotometrically measured Ly α luminosities using NB964 and HSC y -band photometry where Ly α luminosities were derived assuming the NB964 filter’s central wavelength as the line wavelength.

^b In Hu et al. 2021, J100332+020925, J100327+020851, J100339+020747, J100333+020719 and J100337+020736 are known, respectively, by the following IDs: LAE-4, LAE-6, LAE-19, LAE-17 and LAE-18.

pipeline consists of a semi-automated script that applies a list of algorithms to each of the raw exposures. All exposures of the same type (such as arc, tilt) are combined together to construct master calibration frames. For each science exposure, PyPeIt applies the standard reduction techniques including slit edge tracing, wavelength calibration based on arc exposures, flat-field correction and sky subtraction. Typically, PyPeIt performs object extraction and b-spline sky subtraction, jointly. In the end, the pipeline performs both boxcar and optimal extraction to generate the 1D and 2D science spectra.

In order to achieve a higher signal-to-noise, we combined the extracted 1D and 2D spectra for each object in each mask using the coadd script, `pypeit_coadd_2dspec`. Since our targets are expected to be faint sources with

little to no continuum, we chose to perform manual extraction of our sources by providing the spatial-spectral pixel pair for each object in the PyPeIt reduction file.

3. RESULTS

Out of 21 LAE candidates across the two fields, emission lines were detected within the expected wavelength range, based on NB964 filter coverage, in 17 candidates (11 in COSMOS and 6 in WIDE-12). Only one emission line was detected in 15 of these, without any trace of continuum in any of them, whereas each of the remaining two candidates contained two emission lines within the expected wavelength range. The 2D and 1D spectra for these sources are presented in Figures 1 and 2.

We identified the single line in these 15 candidates as Ly α emission at $z \sim 6.9$ and rule out the possibil-

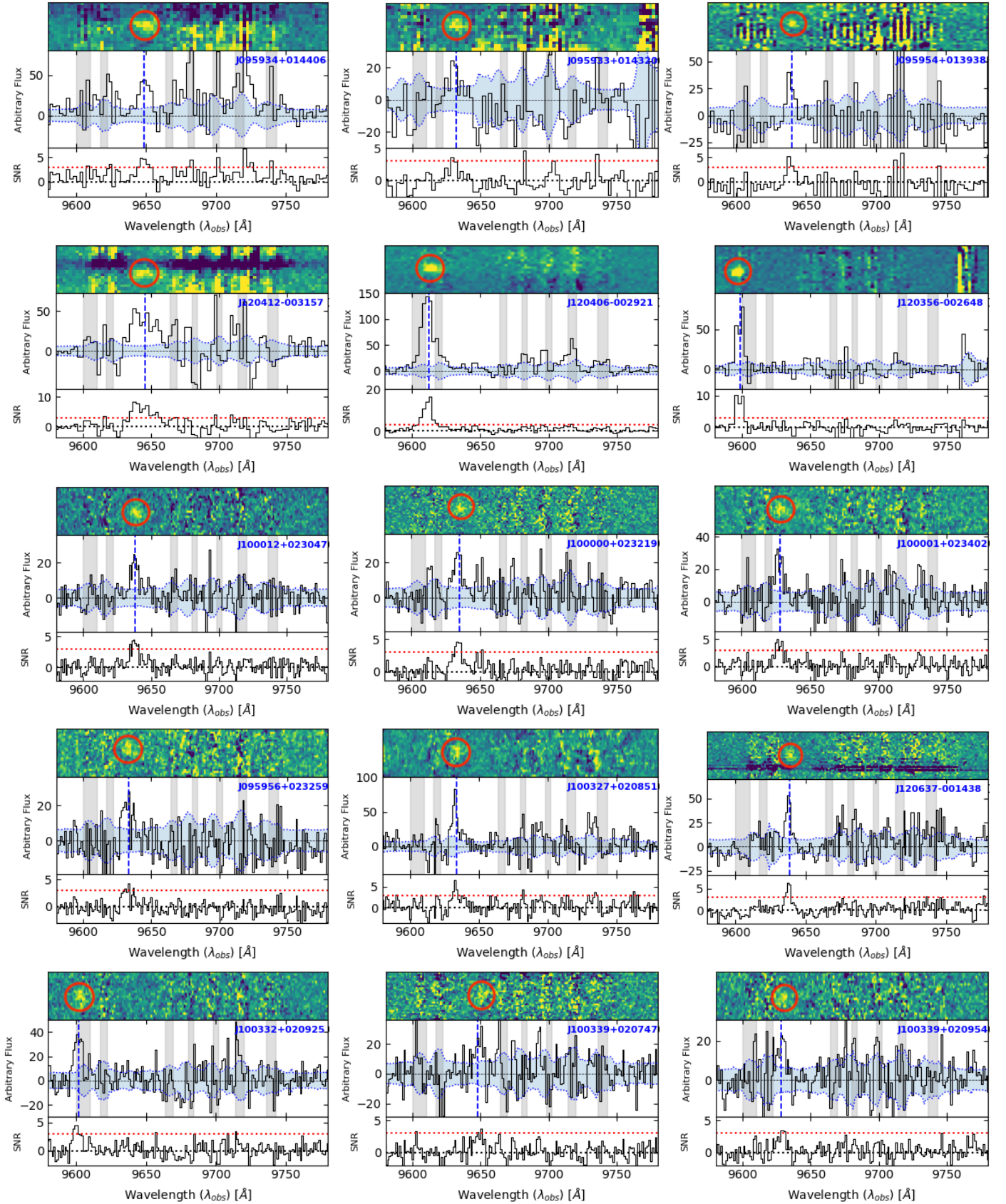


Figure 1. LRIS spectra of confirmed LAGER LAE candidates. The top panel shows the coadded 2D spectrum with detected Ly α emission (red circle). In the middle panel, the coadded 1D spectrum containing the Ly α line (blue line) along with noise spectrum (blue shade) and prominent sky emission regions (gray shade) over-plotted are shown, and the bottom panel is the S/N spectrum with a 3σ limit (red) shown for reference.

ity of being low- z foreground emission for the following reasons: (1) None of these sources are detected in the deep *gri* broad-band images reaching a 5σ depth of $\gtrsim 27.5$ mag in COSMOS and $\gtrsim 26.5$ in WIDE-12. (2) Other prominent rest-frame optical lines can be ruled out as follows: if it were to be $[\text{OIII}]_{\lambda 5007}$ (or $[\text{OIII}]_{\lambda 4959}$), then we should have also detected its complementary line, $[\text{OIII}]_{\lambda 4959}$ (or $[\text{OIII}]_{\lambda 5007}$). If it were to be $\text{H}\alpha$, given LRIS' spectral coverage, then $\text{H}\beta$ and/or $[\text{OIII}]$ should have been detected. Since the detected emission lines are narrow with no obvious double-peak profile, we rule out the possibility of any of them being the $[\text{OII}]_{\lambda\lambda 3727,3729}$ line. (3) Typically, $\text{Ly}\alpha$ emission from star-forming galaxies can be differentiated from other lines based on the asymmetric nature of $\text{Ly}\alpha$ line (e.g. Rhoads et al. 2003). Inspection of 1D spectra in Figure 1 shows a hint of asymmetry in some sources (J120412-003157, J120406-002921, J095934+014406) but owing to the low spectral resolution of LRIS, most other candidates seem to show no significant asymmetry. Considering all the aforementioned evidence, we infer that the detected emission line in these 15 sources is indeed the $\text{Ly}\alpha$ line. Table 2 summarizes the basic properties of all confirmed LAE candidates including their spectroscopic redshifts. Three LAEs (J100332+020925, J100327+020851, J100339+020747) are part of the overdense region in COSMOS, LAGER- $z7\text{OD}1$ (Hu et al. 2019) and have matching confirmations with spectroscopic follow-ups reported by Hu et al. 2021.

Figure 3 shows the color-magnitude diagrams of LAE candidates in COSMOS and WIDE-12 regions. Two LAEs (J120641-001047 and J120636+000959) in WIDE-12 turned out to be $[\text{OIII}]$ emitters where the doublet lines, $[\text{OIII}]_{\lambda 4959}$ and $[\text{OIII}]_{\lambda 5007}$, were detected in both these candidates (Fig. 2). These two sources are not too bright in the NB color-excess ($y - \text{NB}964 < 1.35$).

No emission lines were detected in four candidates (all in COSMOS). However, two of them, J100333+020719 and J100337+020736, were spectroscopically confirmed using Magellan observations in Hu et al. (2021). Based on their derived redshifts, the $\text{Ly}\alpha$ emission is expected at wavelengths $\sim 9624 \text{ \AA}$ and $\sim 9656 \text{ \AA}$, respectively, which coincide with some skylines at these wavelengths. Given that the mask containing these sources had the lowest total integration times compared to other masks, we believe that the non-detections in this mask was due to these two factors combined.

3.1. Non-detection of NV emission

Apart from the $\text{Ly}\alpha$ line, only other UV nebular emission line that we could detect, given the spectral coverage of LRIS, was the $\text{NV}_{\lambda 1240}$. Recent works involving

$z \gtrsim 7$ LAE search have found (tentative) NV detections (e.g. Tilvi et al. 2016; Hu et al. 2017) indicating the presence of a (weak) AGN and possibly metal-rich gas. However, as mentioned earlier, none of our confirmed LAE sources contain any other emission line except $\text{Ly}\alpha$. Therefore, we performed an inverse-variance weighted stack of 1D spectra of all our LAEs to look for NV emission but we found no statistically-significant detection at the expected wavelength (Figure 4). The 2σ upper-limit on the flux ratio of $\text{NV}/\text{Ly}\alpha$ is $f_{\text{NV}}/f_{\text{Ly}\alpha} \lesssim 0.27$, which is consistent with recent findings from studies targeting bright $z \gtrsim 6$ LAEs ($f_{\text{NV}}/f_{\text{Ly}\alpha} < 0.3$; Mainali et al. 2018; Shibuya et al. 2018; Yang et al. 2019).

4. SUMMARY

We report spectroscopic confirmation of 15 LAE candidates from the LAGER survey based on observations using the Keck/LRIS spectrograph. Four of these are the first spectroscopic confirmations of LAE candidates from the WIDE-12 sample. Of the 11 confirmed LAEs in COSMOS, 8 are new confirmations and 3 have matching confirmations with Hu et al. (2021) which is part of the overdense region, LAGER- $z7\text{OD}1$. Overall, including two additional confirmations from previous spectroscopic follow-up using Magellan (Hu et al. 2021), the success rate of LAE confirmations is $\sim 81\%$. We found no significant trace of NV emission, an indicator of AGN activity, in any of these sources. Considering previous LAE confirmations (Hu et al. 2017; Yang et al. 2019; Hu et al. 2021) and those presented in this work, 33 unique LAE sources from LAGER are now spectroscopically confirmed which has more than doubled the sample of spectroscopically confirmed LAE sources at $z \sim 7$.

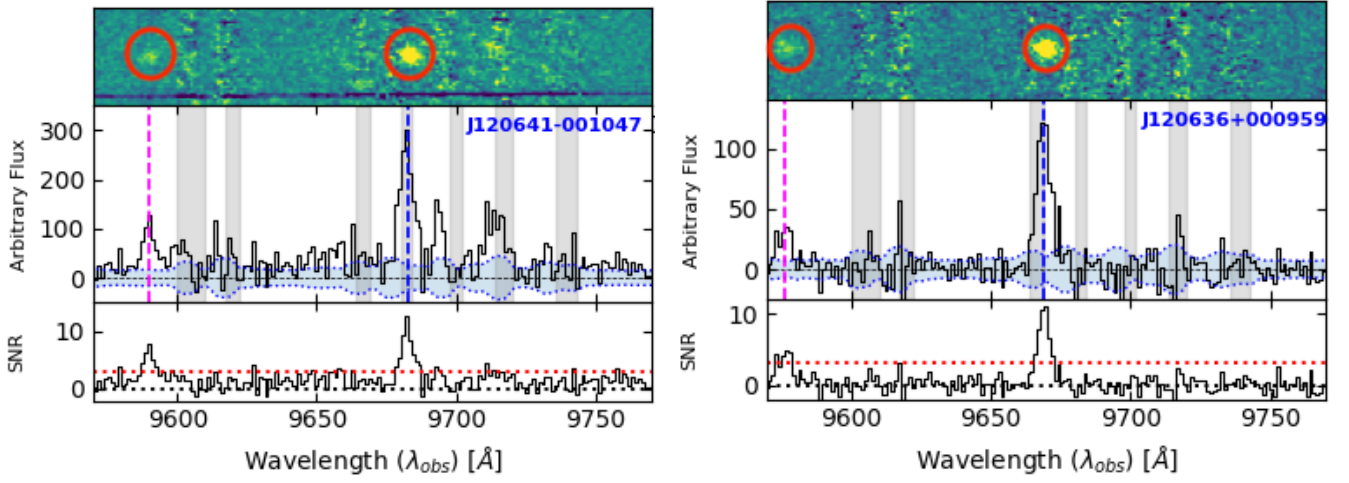


Figure 2. LRIS spectra of two low-redshift interlopers ([OIII] at $z \sim 0.92$). Similar to Figure 1, the coadded 2D (*top*), 1D (*middle*) and S/N (*bottom*) spectra are shown for each source. In the 1D spectrum, the detected [OIII] $_{\lambda 4959}$ (*pink line*) and [OIII] $_{\lambda 5007}$ (*blue line*) emission are also shown.

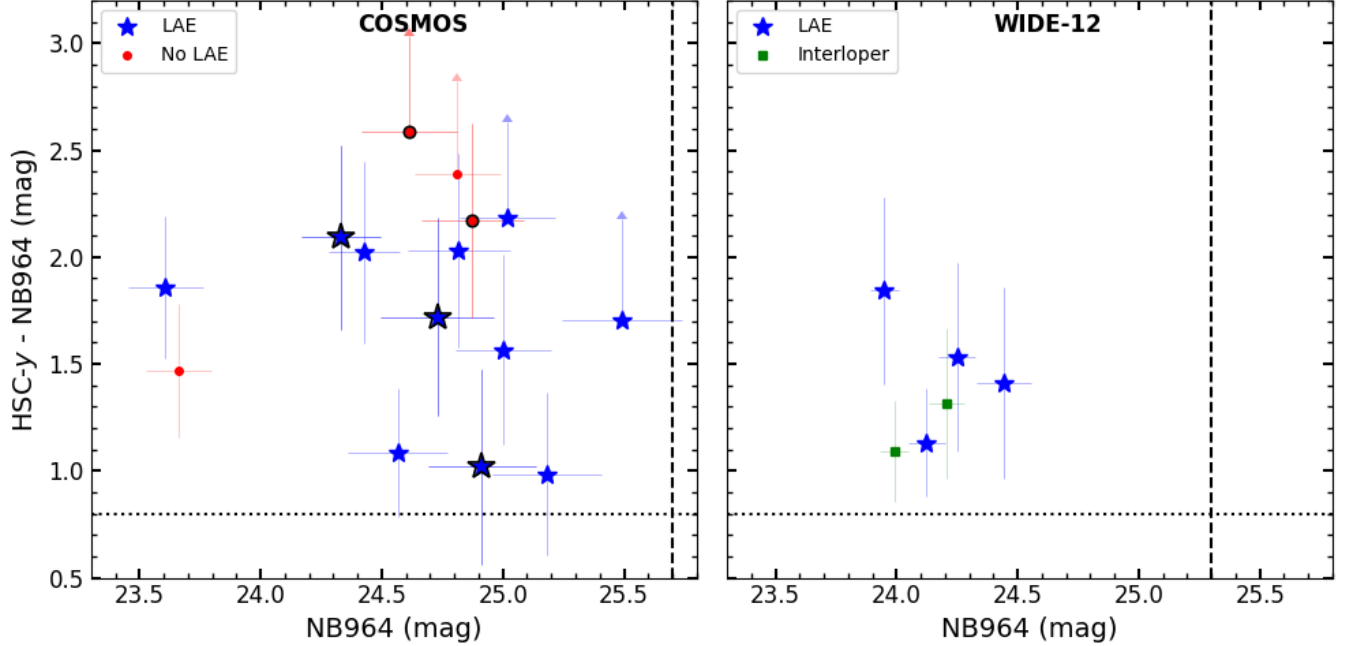


Figure 3. ($y - \text{NB964}$) color as a function of NB964 magnitude for COSMOS (*left*) and WIDE-12 (*right*) regions. In both panels, the color criteria used to select our LAEs (Hu et al. 2019; Wold et al. 2021) are shown for reference: $\text{SNR} > 5$ (*dashed line*) and $y - \text{NB964} > 0.8$ (*dotted line*). Previously confirmed LAEs by Hu et al. 2021 are shown using *black* bordered symbols.

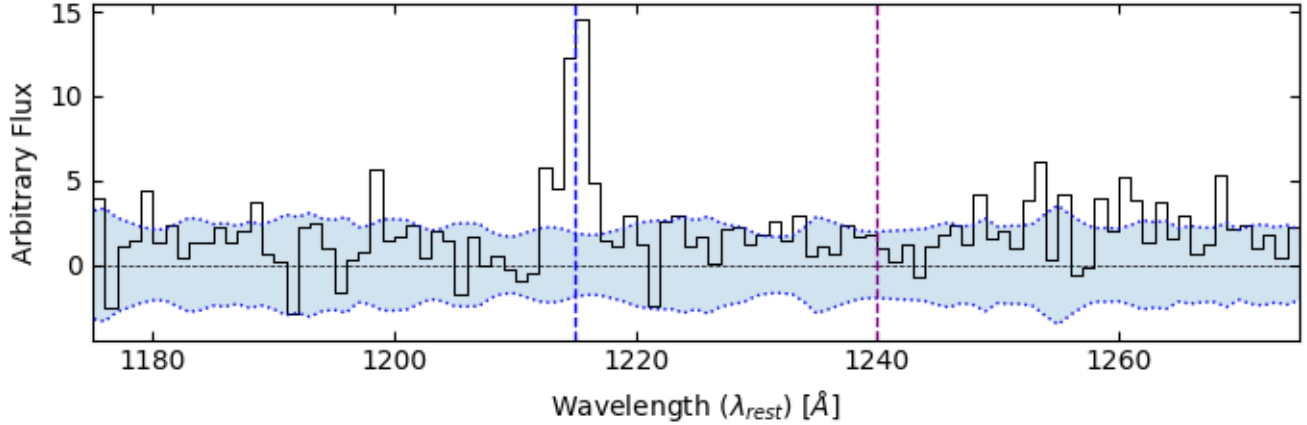


Figure 4. Inverse-variance weighted 1D stack of LAE spectra with the corresponding 1σ error (*blue shade*). No evidence is seen for NV emission that would be expected at a ratio of $f_{NV}/f_{Ly\alpha} > 0.3$, if the $Ly\alpha$ lines were due to AGN. The $Ly\alpha$ (*blue line*) and NV (*purple line*) wavelengths are marked in the spectrum for reference.

1 We thank NASA for its support to ASU via con-
 2 tract NNG16PJ33C, "Studying Cosmic Dawn with
 3 WFIRST". IGBW is supported by an appointment to
 4 the NASA Postdoctoral Program at the Goddard Space
 5 Flight Center, administered by the Universities Space
 6 Research Association through a contract with NASA.
 7 The material is based upon work supported by NASA
 8 under award number 80GSFC21M0002. JW thanks
 9 support from National Natural Science Foundation of
 10 China (grant Nos. 11890693 & 12033006) and the CAS
 11 Frontier Science Key Research Program (QYZDJ-SSW-
 12 SLH006). ZYZ acknowledges support by the National
 13 Science Foundation of China (11773051, 12022303), the
 14 China-Chile Joint Research Fund and the CAS Pioneer
 15 Hundred Talents Program.

16 The data presented herein were obtained at the W. M.
 17 Keck Observatory, which is operated as a scientific part-
 18 nership among the California Institute of Technology,
 19 the University of California and the National Aeronau-
 20 tics and Space Administration. The Observatory was
 21 made possible by the generous financial support of the
 22 W. M. Keck Foundation. The authors wish to recog-
 23 nize and acknowledge the very significant cultural role
 24 and reverence that the summit of Maunakea has always
 25 had within the indigenous Hawaiian community. We are
 26 most fortunate to have the opportunity to conduct ob-
 27 servations from this mountain.

REFERENCES

Castellano, M., Dayal, P., Pentericci, L., et al. 2016, ApJL,
 818, L3, doi: [10.3847/2041-8205/818/1/L3](https://doi.org/10.3847/2041-8205/818/1/L3)

Castellano, M., Pentericci, L., Vanzella, E., et al. 2018,
 ApJL, 863, L3, doi: [10.3847/2041-8213/aad59b](https://doi.org/10.3847/2041-8213/aad59b)

- Dijkstra, M. 2014, PASA, 31, e040, doi: [10.1017/pasa.2014.33](https://doi.org/10.1017/pasa.2014.33)
- Fan, X., Strauss, M. A., Becker, R. H., et al. 2006, AJ, 132, 117, doi: [10.1086/504836](https://doi.org/10.1086/504836)
- Fontana, A., Vanzella, E., Pentericci, L., et al. 2010, ApJL, 725, L205, doi: [10.1088/2041-8205/725/2/L205](https://doi.org/10.1088/2041-8205/725/2/L205)
- Hu, E. M., Cowie, L. L., Barger, A. J., et al. 2010, ApJ, 725, 394, doi: [10.1088/0004-637X/725/1/394](https://doi.org/10.1088/0004-637X/725/1/394)
- Hu, W., Wang, J., Zheng, Z.-Y., et al. 2017, ApJL, 845, L16, doi: [10.3847/2041-8213/aa8401](https://doi.org/10.3847/2041-8213/aa8401)
- . 2019, ApJ, 886, 90, doi: [10.3847/1538-4357/ab4cf4](https://doi.org/10.3847/1538-4357/ab4cf4)
- Hu, W., Wang, J., Infante, L., et al. 2021, Nature Astronomy, 5, 485, doi: [10.1038/s41550-020-01291-y](https://doi.org/10.1038/s41550-020-01291-y)
- Konno, A., Ouchi, M., Ono, Y., et al. 2014, ApJ, 797, 16, doi: [10.1088/0004-637X/797/1/16](https://doi.org/10.1088/0004-637X/797/1/16)
- Konno, A., Ouchi, M., Shibuya, T., et al. 2018, PASJ, 70, S16, doi: [10.1093/pasj/psx131](https://doi.org/10.1093/pasj/psx131)
- Mainali, R., Zitrin, A., Stark, D. P., et al. 2018, MNRAS, 479, 1180, doi: [10.1093/mnras/sty1640](https://doi.org/10.1093/mnras/sty1640)
- Malhotra, S., & Rhoads, J. E. 2004, ApJL, 617, L5, doi: [10.1086/427182](https://doi.org/10.1086/427182)
- . 2006, ApJL, 647, L95, doi: [10.1086/506983](https://doi.org/10.1086/506983)
- Mason, C. A., Fontana, A., Treu, T., et al. 2019, MNRAS, 485, 3947, doi: [10.1093/mnras/stz632](https://doi.org/10.1093/mnras/stz632)
- Oke, J. B., Cohen, J. G., Carr, M., et al. 1995, PASP, 107, 375, doi: [10.1086/133562](https://doi.org/10.1086/133562)
- Ota, K., Iye, M., Kashikawa, N., et al. 2010, ApJ, 722, 803, doi: [10.1088/0004-637X/722/1/803](https://doi.org/10.1088/0004-637X/722/1/803)
- Ouchi, M., Shimasaku, K., Akiyama, M., et al. 2005, ApJL, 620, L1, doi: [10.1086/428499](https://doi.org/10.1086/428499)
- Pentericci, L., Fontana, A., Vanzella, E., et al. 2011, ApJ, 743, 132, doi: [10.1088/0004-637X/743/2/132](https://doi.org/10.1088/0004-637X/743/2/132)
- Pentericci, L., Vanzella, E., Fontana, A., et al. 2014, ApJ, 793, 113, doi: [10.1088/0004-637X/793/2/113](https://doi.org/10.1088/0004-637X/793/2/113)
- Planck Collaboration, Adam, R., Ade, P. A. R., et al. 2016, A&A, 594, A1, doi: [10.1051/0004-6361/201527101](https://doi.org/10.1051/0004-6361/201527101)
- Prochaska, J., Hennawi, J., Westfall, K., et al. 2020a, The Journal of Open Source Software, 5, 2308, doi: [10.21105/joss.02308](https://doi.org/10.21105/joss.02308)
- Prochaska, J. X., Hennawi, J., Cooke, R., et al. 2020b, pypeit/PypeIt: Release 1.0.0, v1.0.0, Zenodo, doi: [10.5281/zenodo.3743493](https://doi.org/10.5281/zenodo.3743493)
- Rhoads, J. E., Dey, A., Malhotra, S., et al. 2003, AJ, 125, 1006, doi: [10.1086/346272](https://doi.org/10.1086/346272)
- Rhoads, J. E., Xu, C., Dawson, S., et al. 2004, ApJ, 611, 59, doi: [10.1086/422094](https://doi.org/10.1086/422094)
- Rockosi, C., Stover, R., Kibrick, R., et al. 2010, in Society of Photo-Optical Instrumentation Engineers (SPIE) Conference Series, Vol. 7735, Ground-based and Airborne Instrumentation for Astronomy III, ed. I. S. McLean, S. K. Ramsay, & H. Takami, 77350R, doi: [10.1117/12.856818](https://doi.org/10.1117/12.856818)
- Shibuya, T., Kashikawa, N., Ota, K., et al. 2012, ApJ, 752, 114, doi: [10.1088/0004-637X/752/2/114](https://doi.org/10.1088/0004-637X/752/2/114)
- Shibuya, T., Ouchi, M., Harikane, Y., et al. 2018, PASJ, 70, S15, doi: [10.1093/pasj/psx107](https://doi.org/10.1093/pasj/psx107)
- Stark, D. P., Ellis, R. S., & Ouchi, M. 2011, ApJL, 728, L2, doi: [10.1088/2041-8205/728/1/L2](https://doi.org/10.1088/2041-8205/728/1/L2)
- Tilvi, V., Pirzkal, N., Malhotra, S., et al. 2016, ApJL, 827, L14, doi: [10.3847/2041-8205/827/1/L14](https://doi.org/10.3847/2041-8205/827/1/L14)
- Trenti, M., Bradley, L. D., Stiavelli, M., et al. 2012, ApJ, 746, 55, doi: [10.1088/0004-637X/746/1/55](https://doi.org/10.1088/0004-637X/746/1/55)
- Treu, T., Schmidt, K. B., Trenti, M., Bradley, L. D., & Stiavelli, M. 2013, ApJL, 775, L29, doi: [10.1088/2041-8205/775/1/L29](https://doi.org/10.1088/2041-8205/775/1/L29)
- Wold, I. G. B., Malhotra, S., Rhoads, J., et al. 2021, arXiv e-prints, arXiv:2105.12191. <https://arxiv.org/abs/2105.12191>
- Yang, H., Infante, L., Rhoads, J. E., et al. 2019, ApJ, 876, 123, doi: [10.3847/1538-4357/ab16ce](https://doi.org/10.3847/1538-4357/ab16ce)
- Zheng, Z.-Y., Malhotra, S., Rhoads, J. E., et al. 2016, ApJS, 226, 23, doi: [10.3847/0067-0049/226/2/23](https://doi.org/10.3847/0067-0049/226/2/23)
- Zheng, Z.-Y., Wang, J., Rhoads, J., et al. 2017, ApJL, 842, L22, doi: [10.3847/2041-8213/aa794f](https://doi.org/10.3847/2041-8213/aa794f)
- Zheng, Z.-Y., Rhoads, J. E., Wang, J.-X., et al. 2019, PASP, 131, 074502, doi: [10.1088/1538-3873/ab1c32](https://doi.org/10.1088/1538-3873/ab1c32)